Korean Journal of Remote Sensing, Vol.17, No.2, 2001, pp.165~181

Reflectance of Geological Media by Using a Field Spectrometer in the Ungsang Area, Kyungsang Basin

Kyung-Kuk Kang*, Kyo-Young Song, Chung-Hyun Ahn***, and Joong-Sun Won***

Department of Earth System Sciences, Yonsei University*

Korea Institute of Geoscience & Mineral Resources**, ETRI/CSTL-Image Processing Department***

Abstract : Using a field spectrometer having a spectral range of 0.4μm~2.5μm with a spectral resolution of 1nm, the researchers measured the reflectance of granite, andesitic rocks, sedimentary rocks, and pyrophyllite ore in the Ungsang area, Kyungsang Basin, South Korea. Spectral characteristics of the geological media were investigated from the analysis. The in-situ measured sites were selected in well exposed rock outcrops. In case of unfavorable weather conditions, rocks were sampled and remeasured under natural solar condition. The reflectance of field data was measured at three sites for granite, six sites for andesitic rock, three sites for sedimentary rocks, and two sites for pyrophyllite ore.

The vibrational absorption bands for pyrophyllite are detected in the spectral range of 2.0μm~2.5μm. The absorption band for granites in study area is not distinctive. The reflectance measured under normal field conditions showed strong absorption at wavelengths of 1.4μm and 1.9μm due to the effect of moisture in the atmosphere. After the bands of 1.4μm and 1.9μm were removed, Hull Quotient method was applied to characterize absorption bands.

The reflectances of field data were calculated to estimate the band ratio corresponding to the Landsat TM and EOS Terra ASTER. The researchers suggest here that the TM band2, band3, band4, and band7 or ASTER band2, band3, band4, and band9 are the best combination for discriminating outcrops. The researchers tested and demonstrated using a Landsat TM image in the study area. For geologic applications, decorrelation stretch is also an effective tool to enhance the exposed rock mass in images.

Key Words : spectrometer, reflectance, absorption band, decorrelation stretch, Ungsang area

1. Introduction

One of the objectives of hyperspectral remote sensing is to detect optical characteristics of the Earth surface with hundreds of spectral bands. By enhancing the spectral resolution specifically in visible and near infrared, the researchers can get more useful information from the hyperspectral remote sensing. At the present time, ASTER payloaded on EOS Terra launched on December 18, 1999, can acquire multi-spectral data. Hyperion that provides 220 channels(400nm~2500nm) on EO-1 spacecraft launched on November 19, 2000 is currently transmitting

Received 10 May 2001 ; Accepted 15 June 2001.

hyperspectral images of the Earth's surface. Orbview-4 that has the capability to acquire hyperspectral imagery of 200 channels(450nm~2500nm) will be launched in this year. ARIES-1(Australian Resource Information and Environment Satellite) for mineral exploration, resource mapping, and environmental monitoring that will provide 128 bands from 400nm to 2500nm is to be launched in 2002.

The data of the field spectrometer have been compiled initially by JPL(Jet Propulsion Laboratory). Goetz *et al.* (1981) suggested the necessity of a high spectral-resolution image to discriminate geological rocks in the Death Valley of California and the cuprite mine of Nevada. Kahle *et al.* (1983) suggested the capability to distinguish silicate rocks by using thermal infrared multispectral scanner(TIMS). NASA/JPL actively proceed researches using AVIRIS (Airborne Visible/Infrared Imaging Spectrometer) that has a spectral resolution of 10nm over the wavelength of 0.4μm~2.5μm. Compared AVIRIS image data with spectrometer reflectance and XRD analysis data, Hook *et al.* (1991) suggested discrimination of buddingtonite, alunite, silica, kaolinite in the cuprite mine in Nevada. Abrams *et al.* (1995) successfully compared the simulated data from the AVIRIS and TIMS image of the spectral ranges of ASTER with reflectances measured by the field spectrometer. Huntington *et al.* (1998) showed a possible application of ARIES-1 to discriminating mineralogical variations developed by hydrothermal alteration. Clark (1999) suggested methods for identifying and mapping materials through spectroscopic remote sensing on the earth using laboratory, field, airborne, and spacecraft spectrometers.

There is a serious lack of field observation using field spectrometer for calibration and validation of hyperspectral studies in Korea. This study aims at investigating the relationship between the chemical composition of typical rocks in the Ungsang area, Kyungsang Basin, and the characteristic absorption bands observed by a ASD spectrometer(FieldSpec). To define the best combination for discriminating rocks, band ratios calculated as spectral bands of Landsat TM and ASTER from field reflectance are compared with a Landsat TM image. Although the researchers are not able to establish a quantitative inversion model with this approach, the researchers at least can suggest an optimal bands selection of the Landsat TM or EOS Terra ASTER for geological studies.

2. Methodology

Because most of the study area is covered with vegetations, the researchers selected exposed outcrops in the wide open area for field reflectance measurements. In cloudy conditions, the researchers sampled rocks to measure them later under sunny conditions again. Reflectances that measured in-situ were analyzed to compare with standard spectral libraries including JHU(John Hopkins University), JPL(Jet Propulsion Laboratory), and USGS(United States Geological Survey). Because the conditions are different in the laboratory and on the field measurement, the researchers try to make a comparative study by using XSPECTRA develped by AMIRA Research project in CSIRO. The XSPECTRA is useful to interpret complicated spectral data that measure in field and to explore mineral resources. First, the bad channels near 1.4μm and 1.9μm effected by atmosphere moisture are eliminated by assigning a "NULL value". Second, on the module of

spectral resampling in XSPECTRA, it is revised to use the module of "spline interpolation". Third, the standard spectral library is compared with field reflectance through the "hull quotient technique", the method of continuum removal, so that it displays common characteristics and absorption bands. Fig. 1 summarizes the processing steps of the analysis. Finally, the researchers can investigate the relationship between the absorption band and the mineral, chemical composition that is measured in each rock.

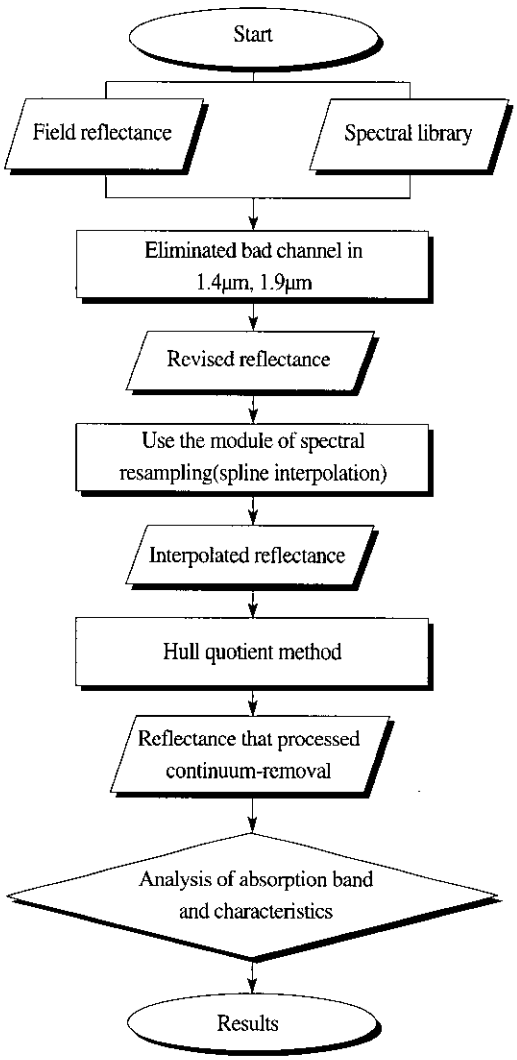

Fig. 1. Flowchart of Hull quotient technique in XSPECTRA.

The field reflectance is then summed over the corresponding bandwidth of Landsat TM and ASTER so that the band ratio is calculated. The estimated band ratios are compared with the actual band ratios of Landsat TM images. Although the Landsat TM image was not acquired simultaneously with the field reflectance, the researchers were still able to show the effective band selection process for geologic application. For Landsat TM image enhancement to discriminate geological rocks, the researchers applied decorrelation stretch method to enhance the color saturation.

3. Spectral Library and Field Reflectance

1) General Description of Study Area

The study area is located at longitude 129°1′ 00″E~129°14′00″E, and 35°17′00″N~35°36′00″N. It covers an area of 19.7km by 35.1km. Geological maps at a scale of 1 to 50,000 include Eonyang, Yangsan and Dongrae in southeastern Korea.

Yangsan and Dongrae faults stretch NNE-SSW direction. The left part of the faults is steeper and higher than the right one and Chunsung-san (881M) and Wonhyo-san(922M) are two peaks in the study area. Both sides of the area that pass across the Yangsan and Dongrae fault, is different in geological facies and terrain.

The study area is composed of lower cretaceous sedimentary rocks of Hayang group, volcanic rocks of Yuchun group, and Bulkuksa granites. Well exposed outcrops found at the top of Chunsung-san, Wonhyo-san, and Cheonbulsan. Ukwang pyrophyllite mine is also developed in

the study area. Sedimentary rocks are weathered due to fault activities, which are composed of mostly reddish brown sandstone and shale. The surface of pyrophyllite ore body shows milky and dark brown color. But ore body developed in Ukwang mine is partly intrusive as greenish gray rock. Gray feldspar porphyry is distributed over the top of Chunsung-san. Wonhyo-san that is composed of andesitic rocks is mainly covered with short shrubbery of brown leaves.

2) Spectral Library

To compare the reflectance that is measured in the study area, three spectral libraries including JHU, JPL, and USGS are used for the reflectance of rocks, vegetation, and minerals in the wavelength of 0.4μm~2.5μm. The spectral library had been compiled by laboratory measurement under a definite illumination and halogen lamp. It must be different from the reflectance that is measured in the field under sunlight. However, absorption characteristics with respect to compositional component should be similar to each other if atmospheric effects are properly removed. The special feature and characteristics of each spectral library is summarized in Table. 1.

(1) Spectral Characteristics of Igneous Rocks

Fig. 2a illustrates measured data of a fresh section for granites in the wavelength of 0.4μm~2.5μm. Absorption features at 1.4μm, 1.9μm, and 2.2μm are typical for Gs1. The absorption bands at 1.4μm and 1.9μm are due to the vibrational processes about the overtone tone and combination tone for water molecules. The absorption band at 2.2μm is owing to the fundamental tone (Elachi, 1987), which is related to the existence of mica that has OH- in rocks.

(2) Andesite

The reflectance of andesite is shown in Fig. 2b. Compared with those of granite, an absorption at 2.2μm band is not seen. As1 and As4 are not shown in the absorption band at 1.9μm. However, As2 has typical absorption bands at 1.4μm, 1.9μm

Table. 1. Characteristics of Spectral Libraries(Clark, 1993; Hook, 1998).

	JHU		JPL		USGS	
wavelength (μm)	Equipment		Equipment		Equipment	
	becknic	0.4~25	beckman	0.4~2.5	perknic	0.4~14.1
	nicolet	2.1~25	nicolet	2.1~5.4		
rocks	· Igneous, Sedimentary, Metamorphic rocks		-		· Igneous, Sedimentary, Metamorphic rocks	
mineral	· Silicate, Carbonate, Sulfate, Oxide, Halide, Hydroxide, Sulfide		· Arsenate, Borate, Sulfate Carbonate, Cyclosilicate Element, Halide, Oxide Hydroxide, Silicate, Sulfide Phosphate, Tungstae		· Borate, Carbonate Chloride, Sulfate	
vegetation	· Conifers, Decidous, mineralDrygrass, Grass		-		· Tree, Vegetation(dry), Grass	
Feature	· Various data about rocks meteorites, manmade, soils, vegetation, water. · Data under condition in powder and solid		· The three different size of power about mineral · 160 minerals		· Precise measurement for minerals · 481 minerals · Various data of same rocks	

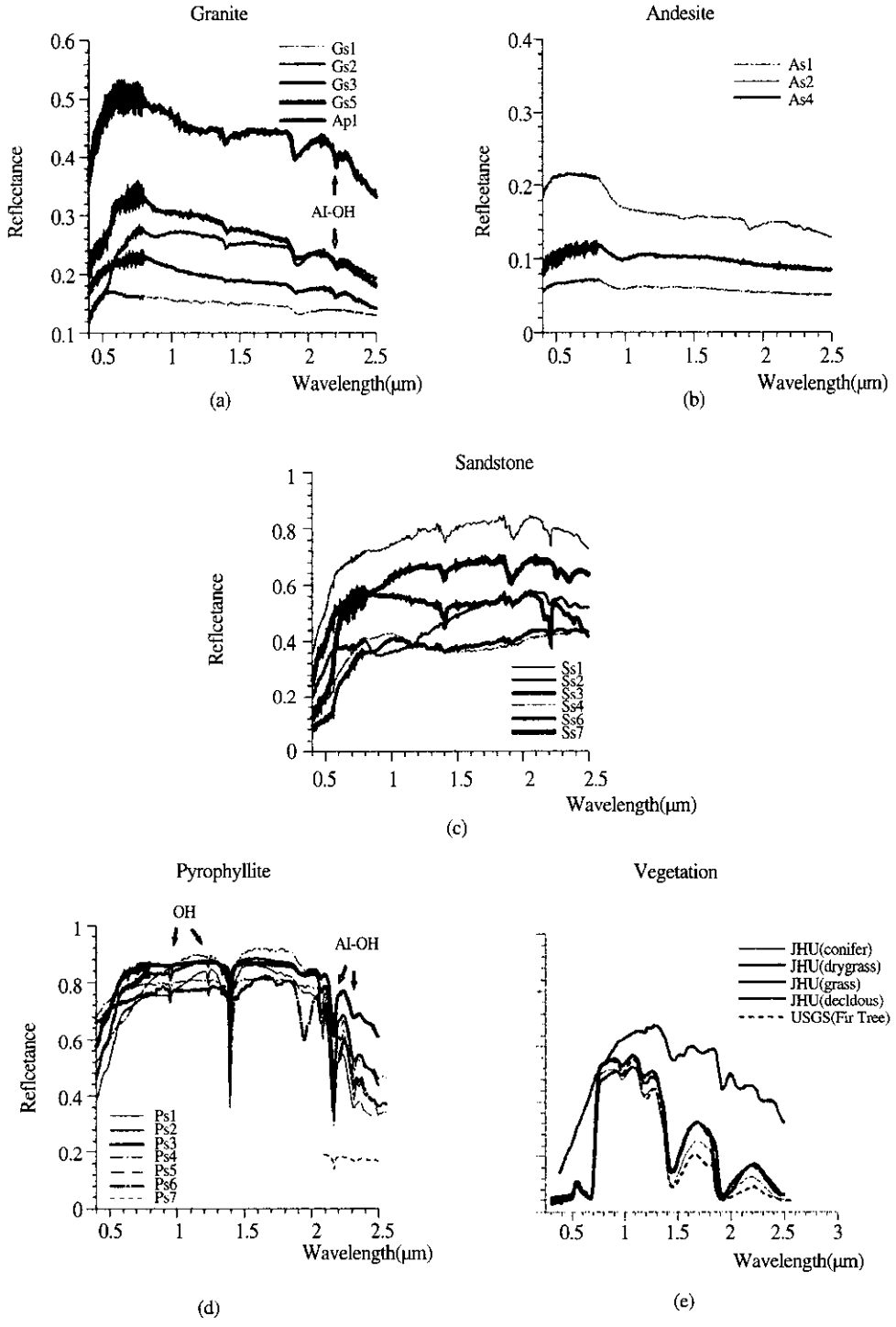

Fig. 2. Reflectances of spectral library:(a)granite (Gs1～Gs5) and aplite(Ap1), (b)andesite (As1, As2, As4), (c)sandstone (Ss1: Arkosic, Ss2: Glaouconite, Ss3: Micaceous, Ss4: Ferruginous, Ss6: Purble banded, Ss7: Red), (d)pyrophyllite (Ps1～Ps3: JPL; Ps4～Ps6: USGS; Ps7: JHU), (e)vegetation; JHU (conifer, decidous, drygrass, grass) and USGS(Fir Tree).

and 2.3μm. Though all are andesites, the existence of the absorption band depends on the minerals and chemical composition. Lack of an absorption band at 1.9μm and 2.0~2.5μm implies that As1 and As4 do not contain water bearing minerals and hydroxyl ions. The reflectance of the spectral library is measured by becknic at JHU using the fresh section of rock sample.

(3) Sandstone

Fig. 2c shows the spectral characteristics of sandstone. The compositional color of sandstone varies with the origin. Therefore, one common spectral library cannot easily be established for sedimentary rocks. Absorption bands exist specially in the wavelength of 2.0μm to 2.5μm. Unlike the granite or andesite case, the sandstone library was established by a becknic measurement at JHU using powder of the size under 75μm(Fig. 2c).

(4) Pyrophyllite($Al_2Si_4O_{10}(OH)_2$)

The typical reflectance of pyrophyllite is illustrated in Fig. 2d. XRD(X-Ray Diffraction) analysis was also performed to measure the particle size reflectance over the same spectral range.

The reflectance of pyrophyllite in the JPL spectral library has with three different patterns based on the particle sizes (125μm~500μm(Ps1), 45μm~125μm(Ps2), <45μm(Ps3)). The smaller the particle size is, the higher the reflectance generally is. In case of USGS spectral library, it is shown as the same pattern according to the particle size (Ps4, Ps5, Ps6).

In the range of SWIR, there is a strong absorption band at 2.16μm and a slightly weak absorption band at 2.3μm, and corresponds to the characteristic of vibrational processes by Al-OH including pyrophyllite (Clark, 1999). The effect of OH- results in weak absorption at 0.9μm, 1.2μm and strong absorption at 1.4μm, but absorption near 1.9μm is absent.

(5) Vegetation

The vegetation is characterized by a cross-over near the wavelength of 0.7μm(Fig. 2e). It also showed that the strong absorption band by water at 1.4μm and 1.9μm. There are other absorption bands at 0.4μm and 0.68μm for chlorophyll and at 0.97μm and 1.19μm for water, and band depth and shape depend upon kinds of vegetation (Kokaly *et al.*, 1998).

3) Field Observation Results

The researchers used a Fieldspec ASD spectrometer for field observation in the study area. This instrument has a capability of 1nm spectral resolution over the wavelength of 0.35μm ~2.5μm. At each in-situ measurement site, the spectrometer must be calibrated as white reference. The sensor should also be in a normal position so that the path radiance error is minimized.

Fig. 3 illustrates the location of in-situ measurement sites over a true color composite Landsat TM5 image, and the site specification is summarized in Table. 2.

(1) Granite

Fig. 4a is the reflectance of Bulkuksa granite in the study area. G1 is the granite in the Unyang amethyst mine where outcrop is well exposed. G2 and G3 are respectively in northern and southern part of Ungsang area. Compared with the spectral library(Fig. 2a), one can see a difference at 1.4μm and 1.9μm in which atmospheric moisture plays an important role in field

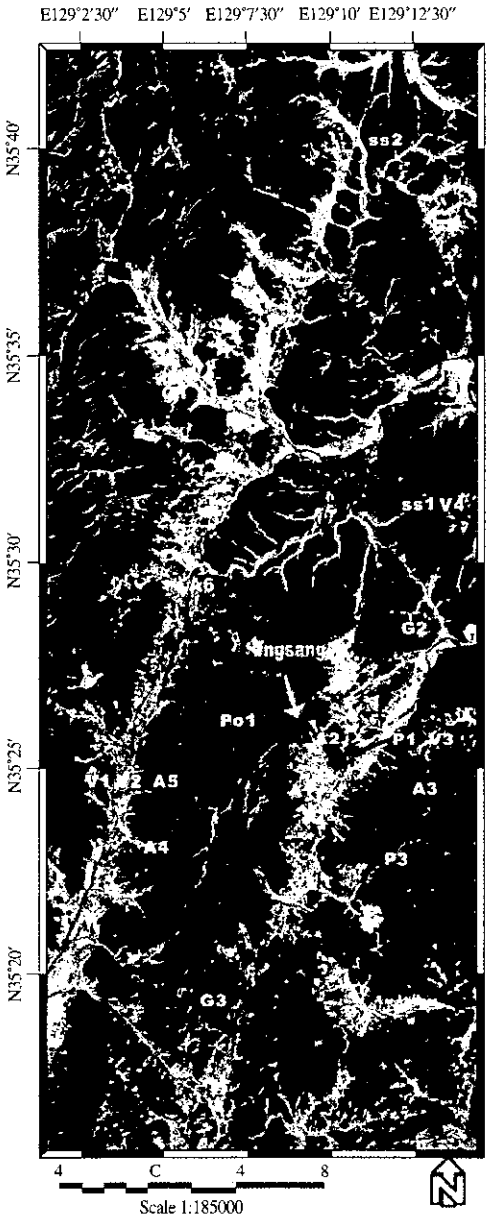

Fig. 3. Location of in situ measurement over true color composite Landsat TM image of the study area.

observation. Moon *et al.* (1998) classified Unyang granite into four types in the Unyang mine, and aplite is the country rock. In Fig. 4a, G1 compiles aplite showing an absorption band at 2.2μm. As compared with the absorption band for the spectral library, the absorption band at 2.2μm for the field measurement can be shown in the effect of Al-OH in mica.

Rock masses of G2, G3 are biotite granite(Kbgr). Principal components minerals are composed of quartz, alkali feldspar(orthoclase, perthite), plagioclase, hornblende, and biotite with accessory components of zircon, anura, and opaqued mineral (Hong *et al.*, 1999). Compared with the spectral library, the overall shape is similar to Gs3, Gs5 around 1.5μm(Fig. 2a), and chemical component is relatively analogous to that.

(2) Andesitic Rocks

Fig. 4b illustrates that A1 and A2 are andesitic rocks on the left section of the Dongrae fault, A3 is on the right part of that. A4 and A5 are the reflectances of tuff breccia measured at the top of Wonhyo-san. Reflectance of A1 and A2 is similar to that of the spectral library about andesite(Fig. 2b), and is a near horizontal line without an absorption band in SWIR.

Po1 is the reflectance of feldspar porphyry nearby the peak of Chunsung-san. Most of the phenocryst are composed of plagioclase with the matrix is of quartz and feldspar, and it results in lack of an absorption band.

(3) Pyrophyllite

Fig. 4c illustrates the reflectance of ore body sampled in Cheonbulsan pyrophyllite mine(P1, P2) and Ukwang mine(P3, P4). P1, P3 are data measured under sunlight in the field, and P2, P4 are ones measured from rock samples under sunny conditions.

The ore in the Chunbulsan mine is composed of quartz, sericite, pyrophyllite as primary minerals and tourmaline, diaspore, and kaolinite as

Table. 2. Summary of field measurement sites.

	Location	Scale	Characteristics	Absorption band
G1	35°32′59″N 129°06′15″E	30m × 100m	a broad distribution horizontally. smooth surface, milky pink rock mass	2.2μm
G2	35°27′10″N 129°11′17″E	Vertical	local distribution, milky rock mass	2.3μm
G3	-	Vertical	milky grey rock mass. poor weathering	2.3μm
A1	-	5m × 5m	erosion, feldspar phenocryst, dark color	-
A2	35°25′06″N 129°07′56″E	Vertical	feldspar phenocryst, dark color outcrop	-
A3	35°23′48″N 129°10′58″E	15m × 20m	erosion, partly brown surface by pyrite	2.34μm
A4	35°23′31″N 129°06′27″E	Vertical	poorly sorting, different grain size	-
A5	35°23′45″N 129°06′26″E	3-5m × 5-10m	rough surface, dark color, well weathering	-
A6	-	5-8m × 15-20m	greenish color, joint system, erosion banded with dark and greenish one	2.32μm
Po1	35°24′42″N 129°07′30″E	10m × 50m	milky grey plagioclase phenocryst joint system, partly existence	-
ss1	35°32′30″N 129°11′24″E	2m × 5m	brown rock mass horizontally banded with shale and sandstone	-
ss2	35°41′15″N 129°12′35″E	Vertical	brown rock mass, the existence by road	-
P1	35°25′16″N 129°10′38″E	100m × 50m	ore body that mixed milky and brown abandoned mine, a lot of pine	2.17μm
P3	35°23′48″N 129°10′31″E	Vertical	dark grey, ore body nearby mine	2.20μm
V1 V2	35°23′45″N 129°06′26″E	-	small tree and brown leaves partly	1.19μm
V3	35°25′16″N 129°10′38″E	-	pine with needle leaves	-
V4	35°32′30″N 129°11′24″E	-	a broad green leaves tree	-

(G:Granite, A:Andesitic rocks, Po1:Feldspar Porphyry, P:Pyrophyllite, V:Vegetation)

secondary minerals. Quartz and sericite are primary minerals for the Ukwang ore(Cheong *et al.*, 1989). The main difference in mineral composition between Chunbulsan and Ukwang ore bodies is the existence of pyrophyllite. With the difference for mineral composition, the absorption band may show unusual pattern in the range of 2.0μm to 2.5μm.

Compared with spectral library which was evaluated by X-ray diffraction(XRD) and was uniform particle size, the absorption band in P1 and P2 near 2.16~2.17μm may account for vibrational processes by Al-OH of pyrophyllite, while P3 and P4 have an absorption at 2.2μm due to Al-OH of sericite.

Band depth measured in ore body varies with degree of mineral concentration. If the depth of an absorption band is to be used for the

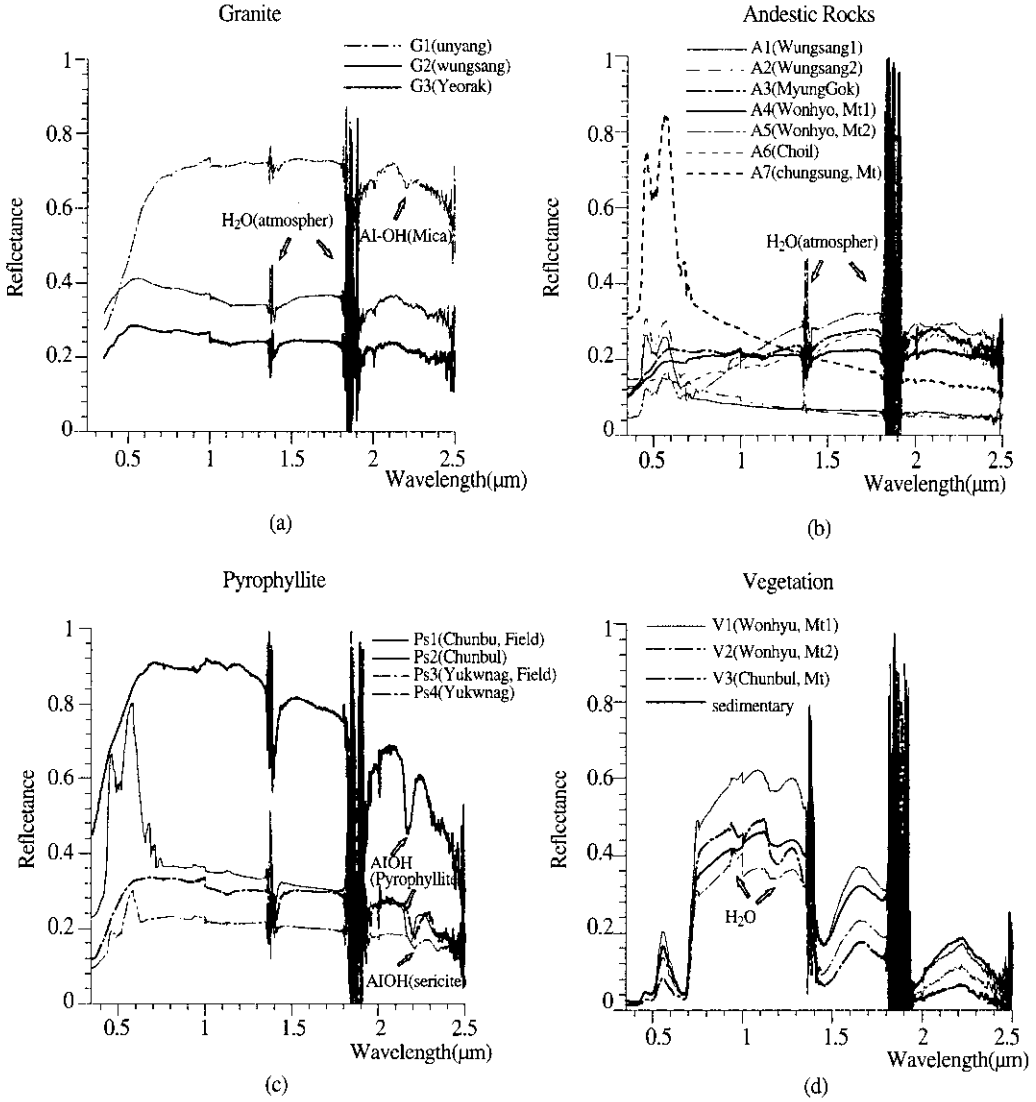

Fig. 4. Field measured reflectances in this study : (a)granite (G1: unyang, G2: wungsang, G3: Yeorak-ri), (b)andesitic rocks (A1, A2: Wungsang, A3: MyungGok-ri, A4, A5: Wonhyo(Mt.), A6: Choil, P1: Chunsung(Mt.)), (c)pyrophyllite ore, and (d)vegetation.

quantification of the substance, the continuum must be removed so that it yields the relative absorption band depth (Kruger *et al.*, 1998). In Fig. 4c, band depth of P1, P2 is higher by 6~15% than that of P3, P4.

(4) Vegetation

In Fig. 4d, V1 and V2 are reflectances of vegetation measured at the top of Wonhyo-san. V3 presents pine nearby Chunbulsan mine, and V4 is of typical vegetation covering sedimentary rocks. As expected the reflectance rapidly increases near 0.7μm. Curves of reflectance for V3 and V4 show the absorption characteristics due to moisture on leaves at 0.97μm and 1.19μm (Kokaly, 1998). The absorption band at 0.68μm is not useful

because of saturation of absorption property near the vegetation (Rowan *et al.* 2000).

4) Comparison of Spectral Library and Field Data

To compare field data with spectral library, we used the XSPECTRA, a mineral mapping package with field spectroscopy developed by CSIRO (Yang *et al.*, 2000). XSPECTRA includes the "hull quotient" method. This algorithm connects upper-convex of reflectance curve so that it makes all wavelengths equal to incident energy (Mason *et al.*, 1997).

First the bands around 1.4μm and 1.9μm are removed using a normalized spectrum (continuum removal) to eliminate atmospheric

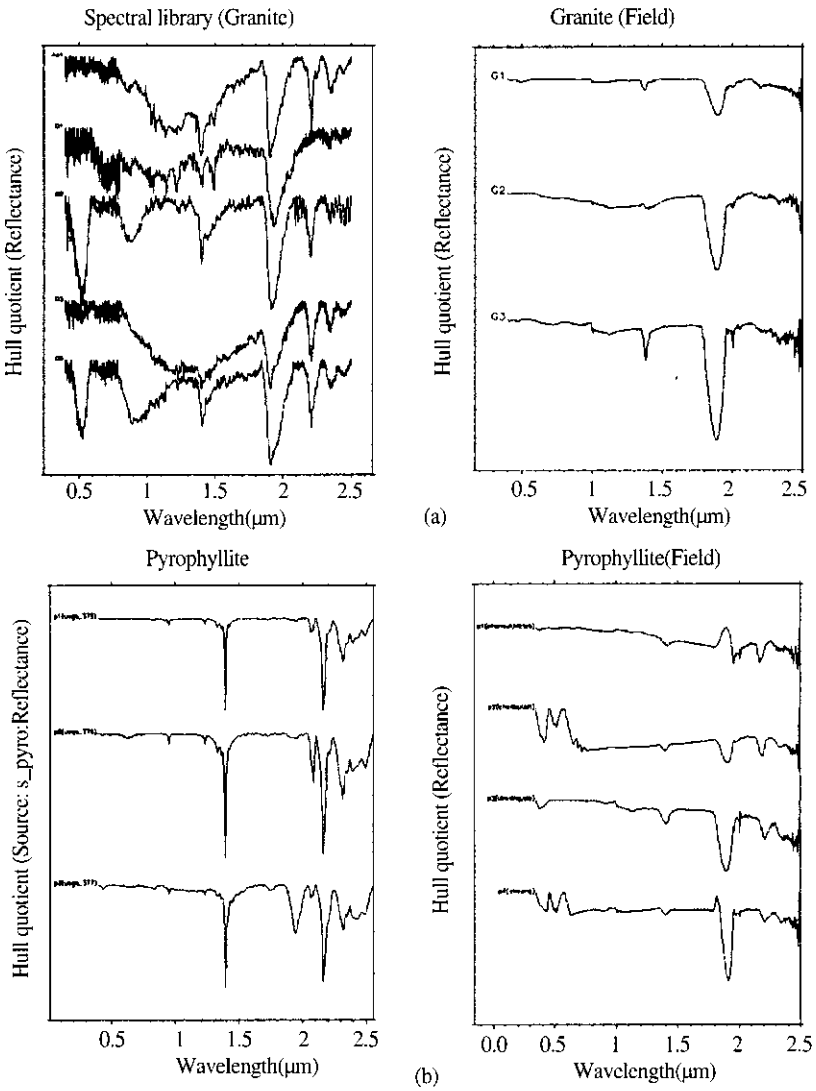

Fig. 5. Hull-quotient spectra of (a)granite and (b)pyrophyllite: The left plots are for spectral library, while the right ones are for field data observed in this study.

Table. 3. Comparison of spectral library and field data.

	Spectral library	Field data
Place	Halogen lamp of definite illumination and supply stable voltage	Measurement in-situ of rock sample under sunlight
spectral range (resolution)	0.4μm~2.5μm (1nm)	0.4μm~2.5μm (1nm)
Condition	Fresh section on rock or powder of regular particle size	In-situ measurement or rock sample from outcrop
Kinds of sample	Igneous rocks, andestic rocks, sandstone, pyrophyllite and vegetation	Granite, andestic rocks, sandstone, pyrophyllite ore and vegetation
Characteristics	The absorption band at 1.4μm and 1.9μm Comparable with data each other due to definite illustration	Incorrect reflectance at 1.4μm and 1.9μm by the atmospheric moisture To be influenced to intensity of source as measured time and altitude of sun
Difference	Because of measurement on fresh section or regular powder Facility to detect absorption band due to mineral in rock	Show the characteristic of reflectance as incident quantity in the range of visible

moisture effects. In case of granite, the left diagram of Fig. 5a indicates the reflectance of spectral library, while the right one does the reflectance of field data. In the right plot of Fig. 5b, only G1 show the very weak absorption band at 2.2μm. However, the granite absorption bands are not distinctive except unyang granite.

Fig. 5b displays reflectance of pyrophyllite spectral library(left) in which strong absorption bands at 1.4μm, 2.17μm, and 2.35μm are noted. In field data(right plot of Fig.5b), absorption at 2.17μm is typical in P1 and P2, Chunbulsan mine pyrophyllite, but not in P3, P4. The differences between the standard spectral library and field data are summarized in Table 3.

5) Absorption band for granite and pyrophyllite

Fig. 6 displays the discriminating capabilities of the multispectral and hyperspectral satellites. In Fig. 6a, the absorption band of granite at 2.2μm can possible be detected by ASTER band 6 or AVIRIS band 193 and 194. The absorption band of pyrophyllite at 2.17μm also corresponds to ASTER band 5 or AVIRIS band 190 and 191. It suggests that AVIRIS and ASTER can possibly be used to discriminate granite and pyrophyllite in this area.

4. Analysis of Field Reflectance and Satellite Image

The Band ratio of spectral bands enhances spectral reflectance differences, to suppress systematic effects such as topography, and to provide a quantitative measure of the spectral information in data(Goetz *et al.* 1981, 1985; Bennett *et al.* 1993; Watson, 1996).

The researchers first simulated the same spectral range of satellite images (Landsat TM and ASTER) using the measured spectral reflectance, and then estimated the band ratio. Since the researchers did not apply atmospheric correction, the results cannot be utilized quantitatively. However, it still provides a useful criterion on selection of optimal bands for geological studies.

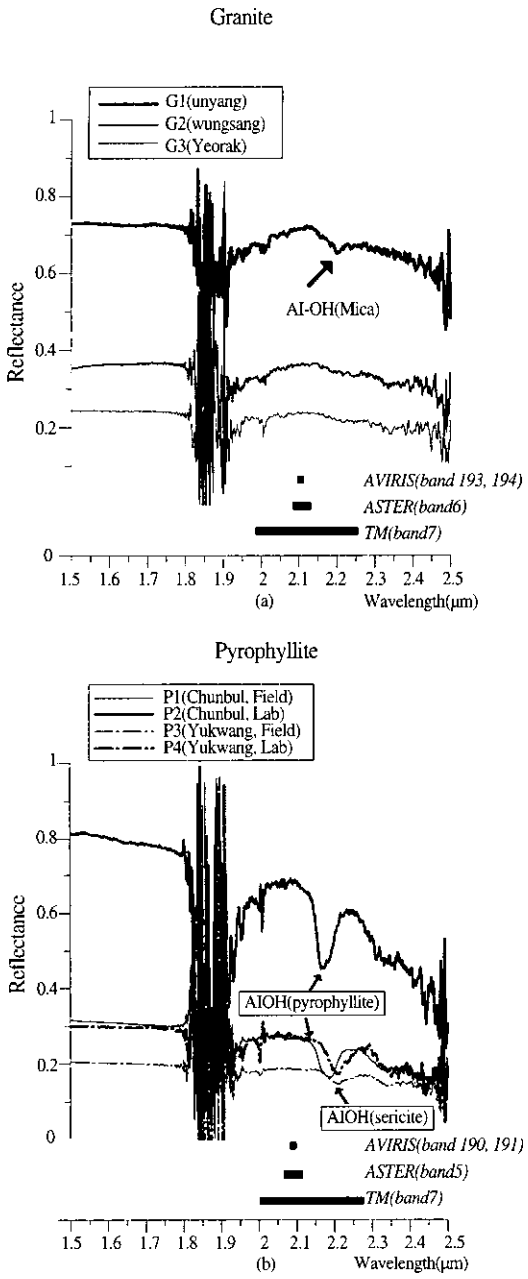

Fig. 6. Absorption band for granite and pyrophyllite.

1) Band Ratio of Spectral Library

As listed in Table. 4, the band ratios of Landsat TM3/TM7, TM4/TM7 are common to all types of granite and andesite. The band ratio of band7/band1 for sandstone shows the highest ratio due to rapidly increased reflectance near visible range(Fig. 2c). Because of absorption in the wavelength of band7(TM), band ratios of band5/band7 and band4/band7 for pyrophyllite show the highest based upon the USGS and JPL spectral library. Band ratios of Ps1, Ps2, and Ps3 are the JPL spectral library, while those of Ps4, Ps5, and Ps6 are the USGS spectral libraries. The two libraries provide similar results.

For ASTER, the granite and andesite would be effectively imaged by the band ratios of band2/band9 and band3/band9, while the band ratios of band4/band9 and band4/band8 considered to be the best for pyrophyllite. In short, the researchers can suggest suggested that the ratios of band3/band7, band4/band7, band5/band7, and band4/band3 are useful to discriminate bedrock outcrop, pyrophyllite, and vegetation in Landsat TM images. The ASTER band ratios of band2/band9, band3/band9, band4/band9, band4/band8, and band3/band2 should be useful candidates for classification of exposed rock outcrops, pyrophyllites and vegetation. However, these results are deduced from spectral libraries which are compiled solely by laboratory measurements. Therefore, satellite images in the real world might be different from the laboratory conditions and results.

2) Band Ratio From Field Data

The band ratios estimated from actual field data must be more useful than those from standard spectral libraries. Granite(G1), andesitic rock(A3, A4), and sedimentary rock show the highest band ratio of TM band5/band1. This characteristic is different from the results of the spectral library. However, the ratio may not be effective for actual satellite image because TM band1 is subject to be

Table. 4. Significant band ratios of spectral library and field data (Landsat TM, ASTER).

Rock Types	Spectral Library						Rock Types	Field Data					
	Landsat TM			ASTER				Landsat TM			ASTER		
	1st	2nd	3rd	1st	2nd	3rd		1st	2nd	3rd	1st	2nd	3rd
Ap1	b3/b7	b2/b7	b3/b5	b2/b9	b3/b9	b1/b9	G1	b5/b1	b4/b1	b7/b1	b4/b1	b3/b1	b5/b1
Gs1	b2/b7	b3/b7	b4/b7	b1/b9	b2/b9	b1/b7	G2	b2/b7	b1/b7	b3/b7	b1/b9	b2/b9	b2/b8
Gs2	b4/b1	b5/b1	b3/b1	b3/b1	b3/b9	b3/b8	G3	b2/b7	b1/b7	b3/b7	b1/b9	b2/b9	b3/b9
Gs3	b4/b7	b3/b7	b2/b7	b3/b9	b2/b9	b3/b8	A1	b2/b7	b1/b7	b2/b5	b1/b9	b1/b8	b1/b7
Gs5	b4/b7	b3/b7	b4/b1	b3/b9	b2/b9	b3/b8	A2	b2/b7	b1/b7	b2/b5	b1/b9	b1/b8	b1/b7
As1	b3/b7	b4/b7	b2/b7	b3/b9	b2/b9	b3/b8	A3	b5/b1	b7/b1	b5/b2	b4/b1	b5/b1	b4/b3
As2	b3/b7	b2/b7	b1/b7	b2/b9	b1/b9	b1/b8	A4	b5/b1	b7/b1	b4/b1	b4/b1	b4/b3	b4/b2
As4	b4/b7	b3/b7	b2/b7	b3/b9	b3/b8	b3/b7	A5	b5/b3	b5/b1	b7/b1	b4/b2	b6/b2	b5/b2
Ss1	b7/b1	b5/b1	b4/b1	b4/b1	b5/b1	b7/b1	A6	b5/b3	b5/b1	b7/b3	b4/b2	b5/b2	b6/b2
Ss2	b7/b1	b5/b1	b7/b2	b5/b1	b7/b1	b5/b1	Po1	b2/b7	b1/b7	b2/b5	b1/b9	b1/b8	b1/b7
Ss3	b7/b1	b5/b1	b4/b1	b7/b1	b9/b1	b5/b1	sh1	b5/b1	b4/b1	b3/b1	b3/b1	b4/b1	b3/b9
Ss4	b7/b1	b4/b1	b5/b1	b9/b1	b8/b1	b7/b1	ss3	b4/b1	b5/b1	b7/b1	b3/b1	b4/b1	b5/b1
Ss6	b4/b1	b5/b1	b3/b1	b3/b6	b3/b9	b3/b1	ss1	b5/b3	b5/b1	b4/b3	b4/b2	b5/b2	b6/b2
Ss7	b5/b1	b7/b1	b4/b1	b5/b1	b4/b1	b6/b1	ss2	b4/b1	b7/b1	b5/b1	b3/b1	b5/b1	b7/b1
Ps1	b5/b7	b4/b7	b3/b7	b4/b5	b3/b5	b4/b9	P1	b2/b7	b2/b5	b1/b7	b1/b9	b1/b8	b1/b6
Ps2	b5/b7	b4/b7	b3/b7	b4/b9	b4/b5	b4/b8	P2	b4/b7	b3/b7	b2/b7	b3/b9	b2/b9	b3/b8
Ps3	b5/b7	b4/b7	b3/b7	b4/b9	b4/b8	b4/b5	P3	b2/b7	b2/b1	b3/b7	b1/b9	b1/b8	b1/b6
Ps4	b5/b7	b4/b7	b3/b7	b4/b9	b4/b8	b4/b5	P4	b3/b7	b4/b7	b2/b7	b2/b9	b3/b9	b2/b8
Ps5	b5/b7	b5/b1	b4/b7	b4/b9	b4/b8	b4/b5	V1	b4/b1	b4/b3	b5/b1	b3/b2	b4/b2	b3/b9
Ps6	b5/b7	b4/b7	b3/b7	b4/b9	b4/b8	b3/b9	V2	b4/b3	b4/b1	b5/b3	b3/b2	b3/b9	b4/b9
Conifer	b4/b3	b4/b1	b4/b2	b3/b2	b3/b9	b3/b1	V3	b4/b1	b4/b3	b4/b7	b3/b9	b3/b2	b3/b8
decidous	b4/b3	b4/b1	b4/b2	b3/b2	b3/b9	b4/b2	V4	b4/b1	b4/b3	b5/b1	b3/b2	b4/b2	b3/b9
grass	b4/b1	b4/b3	b5/b1	b3/b2	b4/b2	b3/b1							

effected by haze. The band ratio of band2/band7 is general effective for rocks and pyrophyllite, and band4/band3 for vegetation(Table. 4).

For ASTER, the useful band ratio for granite(G2, G3) is band2/band9, and those of andesitic rocks are band4/band2 and band4/band3. The ratios of band2/band9 and band3/band9 might be good for pyrophyllite detection and it can be explained by the absorption band in 2.0μm~2.5μm. Compared with the band ratio of Landsat TM in Table 4, the effective band ratios of ASTER apparently have more various options than those of Landsat TM. SWIR spectral ranges of ASTER band5 - band9 are about 40nm to 70nm, while Landsat TM band7 is 270nm in bandwidth.

Based upon field measurement, the researchers suggest that band2/band7, band3/band7, and band4/band3 for Landsat TM are effective to discriminate rocks from surrounding vegetation. When one uses ASTER image, band2/band9, band3/band9, band4/band2, band3/band2 are good for classification of rock and vegetation.

3) Analysis of Satellite Image Data (Landsat TM)

Since satellite image data are recorded differently in time, solar elevation, condition of atmosphere, aspect and slope of topography, and earth surface(Robinove, 1982), DN values should be converted into radiance or reflectance for comparisons.

The formula that converts DN into radiance or reflectance is given by (Robinove, 1982):

$$Radiance = \frac{DN}{DN_{max}}(L_{\lambda max} - L_{\lambda min}) + L_{\lambda min} \quad (1)$$

DN : the digital value of a pixel from data;
DN_{max} : the maximum digital number;
$L_{\lambda max}$: radiance measured at detector saturation in $mWcm^{-2}sr^{-1}$;
$L_{\lambda max}$: lowest radiance measured by detector in $mWcm^{-2}sr^{-1}$.

$$Reflectance = \frac{\pi}{E\sin(\frac{\alpha * 2 * \pi}{360})}\left[\frac{(DN - Haze_i)}{DN_{max}}\right.$$

$$\left.(L_{\lambda max} - L_{\lambda min}) + L_{\lambda min}\right] \quad (2)$$

E : irradiance in $mWcm^{-2}$ at the top of the atmosphere;
α : solar elevation as annotated on Landsat images;
$Haze_i$: atmospheric haze correction.

$L_{\lambda max}$, $L_{\lambda min}$, E are sensor specified values. Hazei is the value of atmospheric correction for a satellite image. For atmospheric correction, Chavez(1989) suggested a dark-object method.

The researchers selected regions of well developed outcrop in the study area. Geographic location was determined by potable GPS to find exact the corresponding pixel in an image. The researchers calculated the DN from satellite image into radiance and reflectance, and the results are in Table 5. Although there are large time gap between the field survey and Landsat TM image acquisition, geologic conditions are assumed to be stable for a relative by long time. Therefore, the direct comparison of field data and Landsat TM is meaningful to select appropriate bands for geologic application.

The researchers computed band ratios from the reflectance of TM image as in Table 5. Compared with the results from field reflectances, the effective band ratio of TM image is slightly different. It can be explained by two possible effects: one is its scale difference between TM IFOV and field spectrum; and the other is atmospheric effect.

Table. 5. DN, radiance, reflectance, and Max band ratio of Landsat TM for granite, feldspar porphyry, and pyrophyllite (G1:granite, A3,A5:andesitic rocks, Po1(feldspar porphyry), P1(pyrophyllite ore)).

DN	G1	A3	A5	Po1(fpy)	P1
b1	49	54	56	52	55
b2	17	20	21	17	22
b3	15	20	26	18	24
b4	52	25	32	19	62
b5	34	28	64	22	54
b7	9	11	28	11	16
Radiance					
b1	2.8019	3.1032	3.2236	2.9827	3.1634
b2	1.7171	2.0695	2.1870	1.7171	2.3045
b3	1.0888	1.4919	1.9755	1.3306	1.8143
b4	4.0852	1.8859	2.4561	1.3972	4.8997
b5	0.3305	0.2656	0.6547	0.2008	0.5466
b7	0.0363	0.0477	0.1445	0.0477	0.0762
Reflectance					
b1	0.0122	0.0216	0.0253	0.0178	0.0235
b2	0.0250	0.0368	0.0407	0.0250	0.0447
b3	0.0205	0.0363	0.0552	0.0300	0.0489
b4	0.2365	0.1084	0.1416	0.0799	0.2840
b5	0.1095	0.0915	0.1997	0.0734	0.1696
b7	0.0496	0.0589	0.1382	0.0589	0.0822
Max band ratio					
1st	b4/b1	b4/b1	b5/b1	b4/b1	b4/b1
2nd	b4/b3	b5/b1	b4/b1	b5/b1	b5/b1
3rd	b4/b2	b4/b3	b7/b1	b7/b1	b4/b2

Fig. 7a illustrates the color composite image of TM band 3, 4, and 7, in which Ungsang is centered. To enhance geologic features, the researchers applied decorrelation stretch algorithm as in Fig. 7b. Although the top of Wonhyo-san and Chunsung-san are covered with vegetation in early November, the exposed outcrops are well imaged with this band combination after decorrelation stretch.

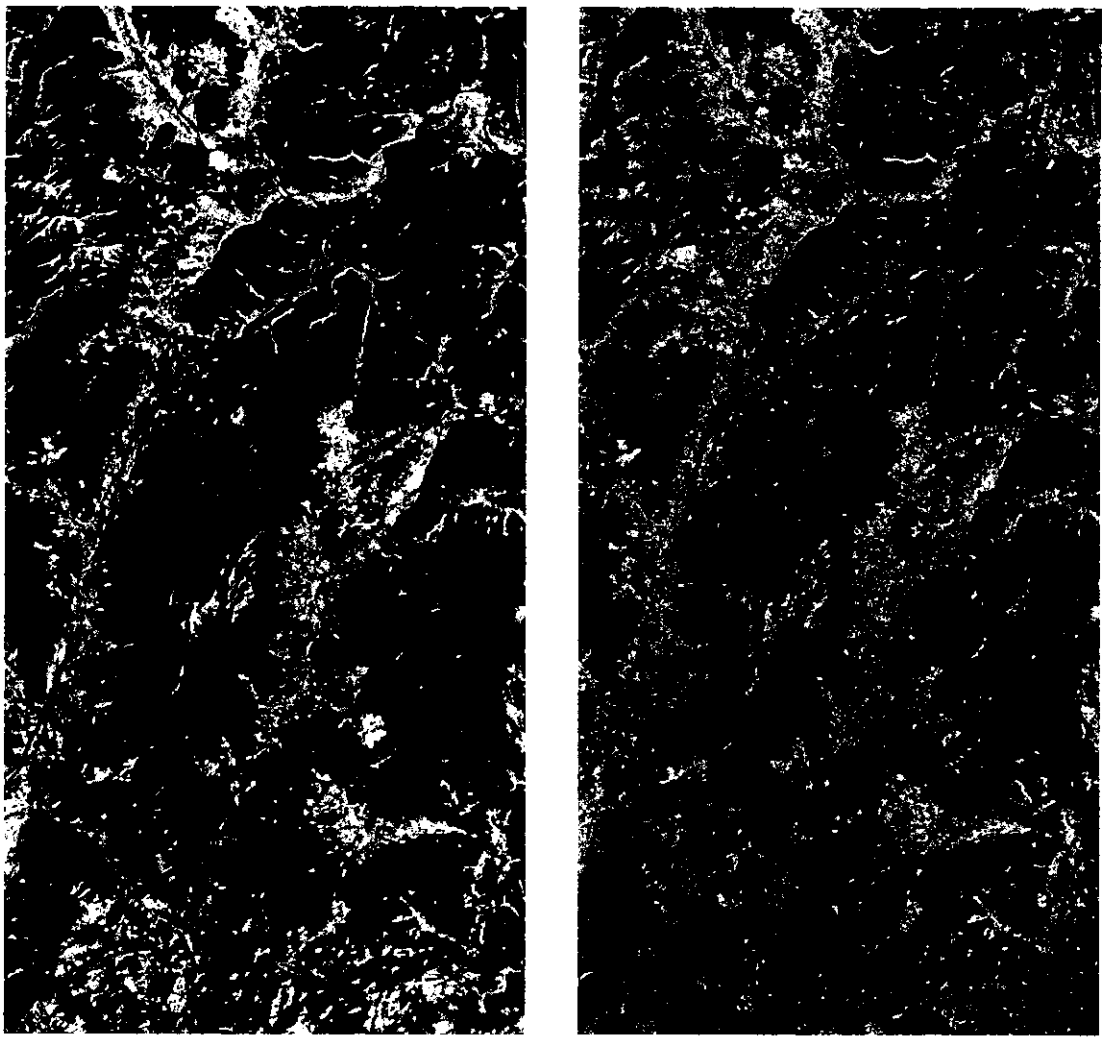

(a) (b)

Fig. 7. (a) Color composite Landsat TM (Nov. 4, 1995) image and (b) Decorrelation stretched image.

4) Analysis of Ratios

From spectral library, the ratio of TM band3/band7 and band4/band7 and the ratio of ASTER band3/band9 and band2/band9 are effective for granite. Based upon field observation, the ASTER band ratios of band1/band9 and band2/band9, however, show more effective results.

Andesite in TM or ASTER image can be enhanced by similar combination of ratio images used for granite. TM band ratios of band5/band1 and band7/band1 are commonly effective in field data and actual TM image analysis.

For pyrophyllite, TM ratios of band5/band7 and band4/band7 show the highest and ratios of ASTER band4/band9 and band4/band8 show the highest in spectral library. But the ratios of field data show differently as effective ratios of TM band2/band7 and ASTER band2/band9 and band3/band9.

5. Conclusions and Discussions

To compile field spectral measurement data in the range of 0.4μm~2.5μm, the researchers have carried out the field spectrometer measurement on various rocks exposed as continuous outcrop in Ungsang-Yangsan-Unyang areas, Kyungsang Basin. Although there already exist standard spectral libraries for typical geologic mass, in-situ field spectrometer data are invaluable to establish spectral database in a certain region for future quantitative studies.

Absorption bands of pyrophyllite in Chunbulsan and Ukwang mine are distinguishable at 2.17μm and 2.2μm. Absorption bands for granite and andesite rocks are not so significant as expected. The Hull Quotient method of XSPECTRA is effective to compare with the absorption band of spectral library and field spectrometer data. The estimated band ratios show that exposed rock can be effectively detected by Landsat TM band2/band7, band3/band7, and band4/band3 or a band ratios of EOS Terra ASTER band2/band9, band3/band9, band4/band2, and band3/band2. To detect exposed rocks, band combination of TM band2, band3, band4, and band7 or ASTER band2, band3, band4, and band9 are suggested. For geologic applications, decorrelation stretch is an effective tool to enhance the exposed rocks mass. The field spectrometer data obtained in this study can be used for validation of ASTER multi-spectral or other hyperspectral observations.

Although the researchers were permitted to acquire ASTER images over the study area by ERSDAC (ASTER ARO#99), no observation has been carried out by EOS Terra ASTER up to data. As soon as ASTER images are to be acquired, the researchers will proceed the comparison of ASTER images and field reflectances. MASTER images by JPL AIRSAR system were not acquired on the field survey because of unfavorable cloudy condition.

Each pixel of the satellite image that includes exposed area is affected by vegetation to some extent and these spectral characteristics near rock mass are largely influenced by the seasonal change of vegetation. For instance, the ratio of TM band4/band1(Table. 5) shows the highest ratio although it is not expected by field observation. Accurate atmospheric correction is also an another obstacle to be managed.

Acknowledgements

The field spectrometer(Fieldspec) was cordially offered by ETRI(Electronics and Telecommunications Research Institute) of Korea, and the XSPECTRA was provided by Peter Mason at MMTG(Mineral Mapping Technologies Group) in CSIRO of Australia.

References

Abrams, M. and S.J. Hook, 1995. Simulated Aster Data for Geologic Studies, *IEEE Trans. Geosci., Remote Sensing*, 33(3):692-699.

Bennett, S.A., W.W. Atkinson, Jr., F.A. Kruse, 1993. Use of Thematic Mapper imagery to identify Mineralization in the Santa District, Sonora, Mexico, *International Geology Review*, 35:1009-1029.

Chavez, P. S., Jr., 1989. Radiometric calibration of Landsat Thematic Mapper multispectral images, *Photogrammetric Engineering and Remote Sensing*, 55(9):1285-1294.

Cheong, Y.W., and Chon, H.T., 1989. Geochemistry of Pyrophyllite Deposits in Yangsan-

Milyang Areas in Korea, *Journal of Korean Inst. Mining Geol*, 22(3):341-354.

Clark, R.N., 1999. Spectroscopy of Rocks and Minerals, and Principles of Spectroscopy, *Manual of Remote Sensing*, John Wiley and Sons Inc, A. Rencz. Editor, New York.

Elachi, C., 1987. *Introduction to the physics and techniques of remote sensing*, John Wiely & Sons, 45-141.

Goetz, A.F.H. and L.C. Rowan, 1981. Geologic Remote Sensing, *Science*, 211:210-212.

Goetz, A.F.H., Vane, G., Solomon, J.E., and B.N. Rock, 1985. Imaging Spectrometry for Earth Remote Sensing, *Science*, 228:1147-1153.

Hong, S.H., Song, K.Y., Kim, Y.B., Kim, B.C., Kim, J.C., and Hwang, J.H., 1999. Geological Report and Map of the Samho sheet (1:25,000), *KIGAM*, DAEJEON, KOREA

Hook, S.J., Elvidge, C.D., Rast, M., and H., Watanabe, 1991. An evaluation of short-wave-infrared (SWIR) data from the AVIRIS and GEOSCAN instruments for mineralogical mapping at Cuprite. Nevada, *Geophysics*, 56(9):1432-1440.

Hook, S.J., 1998. ASTER Spectral Library: *http://speclib.jpl.nasa.gov /reference/summary/ index.htm.*

Huntington, J.F., 1998. Validation of mineralogical variations evident in simulated ARIES-1 hyperspectral data, *Proceedings of SPIE*, 3502:76-86.

Kahle, A.B. and A.F.H. Goetz, 1983. Mineralogic Information from a New Airborne Thermal Infrared Multispectral Scanner, *Science*, 222:24-27.

Kokaly, R. F., Clark, R. N., and Livo, K. E., 1998. Mapping the Biology and Mineralogy of Yellowstone National Park using Imaging Spectroscopy, *Summaries of the 7th Annual JPL Airborne Earth Science Workshop*, 245-254.

Kruger, G., Erzinger, J., and H. Kaufmann, 1998. Laboratory and airborne reflectance spectroscopic analyses of lignite overburden dumps: *Journal of Geochemical Exploration*, 64:47-65.

Mason, P. and Berman, M., 1997. XSPECTRA REFERENCE MANUAL, Exploration and Mining Report 418R, *CSIRO/AMIRA Project P435*, Mineral Mapping with Field Spectroscopy for Exploration.

Moon, S.H., Park, H.I., Ripley, E.M., and Hur, S.D., 1998. Petrochemistry and stable isotopes of granites around the Eonyang rock crystal deposits, *Journal of the Geological society of korea*, 34(3):211-227.

Robinove, C.J., 1982. Computation of physical values for Landsat digital data, *Photogrammetric Engineering and Remote Sensing*, 48:781-784.

Rowan, L.C. Crowley, J.K. Schmidt, R.G. Ager, C.M. and J.C. Mars, 2000. Mapping hydrothermally altered rocks by analyzing hyperspectral image (AVIRIS) data of forested areas in the Southeastern United of States, *Journal of Geochemical Exploration*, 68:145-166.

Watson, K., Rowan, L.C., Browers, T.L., Anton-Pacheco, C., Gumiel, P., and S.H. Miller, 1996. Lithologic analysis from multispectral thermal infrared data of the alkalic rock complex at Iron Hill, Colorado, *Geophysics*, 61(3):706-721.

Yang, K. Hungtington, J. F., Browne, P. R. L., and Ma, C., 2000. An infrared spectral reflectance study of hydrothermal alteration minerals from the Te Mihi sector of the Wairakei geothermal system, New Zealand: *Geothermics*, 29:377-392.